Cite as: Parisi F., De Luca F., Petruzzelli F., De Risi R., Chioccarelli E., Iervolino I. (2012), *Field inspection after the May 20th and 29th 2012 Emilia-Romagna earthquakes*, available at http://www.reluis.it.

# Field inspection after the May 20th and 29th 2012 Emilia-Romagna earthquakes

Fulvio Parisi, Flavia De Luca, Fabio Petruzzelli, Raffaele De Risi, Eugenio Chioccarelli, Iunio Iervolino

fulvio.parisi@unina.it, flavia.deluca@unina.it, fabio.petruzzelli@unina.it, raffaele.derisi@unina.it, eugenio.chioccarelli@unina.it, iunio.iervolino@unina.it

*Dipartimento di Ingegneria Strutturale, Università degli Studi di Napoli Federico II*

## Index

# 1. Introduction

An earthquake cluster with two magnitude peaks on May 20$^{th}$ (Mw 6.0) and May 29$^{th}$ (Mw 5.8), 2012 (moment magnitudes estimated by USGS), hit the Emilia Romagna region (northern Italy). This document reports about some typical damages observed for both modern and historical buildings in the affected area (July 2012). Failure modes observed on existing structures appear compatible with those expected when non-modern seismic design is enforced (e.g., element poor detailing, lacking or ineffective connections, lack of structural robustness and redundancy). Some of these weaknesses are shown in the following for masonry buildings, precast RC structures and ordinary RC structures.

Figure 1.1 shows the surveys locations for the different observed structures where: masonry structures are marked with cyan tags and the MB (Masonry Building) abbreviation; RC precast buildings are marked with green tags and the PCB (Precast Building) abbreviation; and ordinary RC buildings are marked with magenta tags and the RCB (Reinforced Concrete Building) abbreviation. Numbers after the abbreviation (e.g., 2.1) indicate the section in which damages are described. Bracketed letters (e.g., (a)) indicate the order by which the buildings are listed in the sub-sections. Capital letter C after the MB abbreviation refers to churches. In Figure 1.1 the epicentres of the mainshocks that struck the Emilia Romagna region on May 20$^{th}$ and 29$^{th}$, 2012, are also shown.

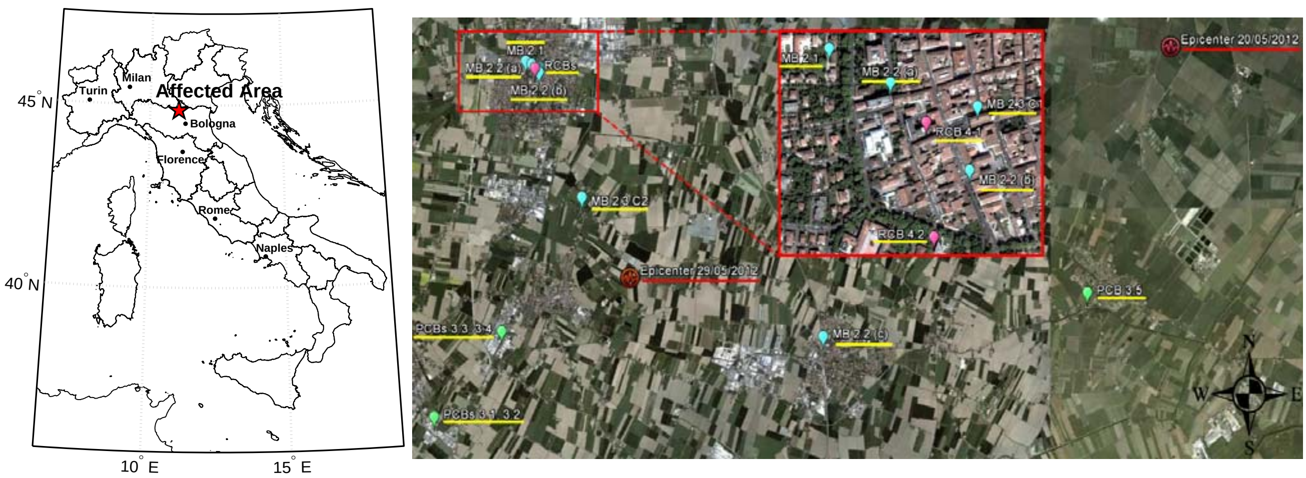


(a) (b)

**Figure 1.1.** (a) Localization of the affected area and (b) GPS localization of the surveys (Cyan tags: Masonry Buildings, Green tags: Precast RC Buildings; Magenta tags: ordinary RC buildings).

The inspected structures are located in the municipalities of Cavezzo, Finale Emilia, Medolla, Mirandola and San Felice sul Panaro, which fall in the Modena province. To provide a better understanding of the earthquake damage, the locations of surveyed sites have been superimposed on shaking maps provided by *Istituto Nazionale di Geofisica e Vulcanologia* (INGV) [http://shakemap.rm.ingv.it/shake/index.html]. Such maps are plotted for both mainshocks in terms of peak ground acceleration (PGA) (Figure 1.2) and spectral acceleration ($S_a$) at vibration periods equal to 0.3, 1 and 3 s (Figures 1.3 to 1.5). PGA values and spectral accelerations at 0.3, 1 and 3 s, computed for the surveyed buildings through shake maps are outlined in Table 1. The latter demonstrates that buildings located in the affected region were subjected to PGA values not lower than 0.2*g* during the two mainshocks.

**Table 1.** PGA and spectral accelerations computed for the inspected buildings through shake maps.

| | | | *May 20th 2012 event* | | | | *May 29th 2012 event* | | | |
|---|---|---|---|---|---|---|---|---|---|---|
| **building ID** [-] | **Lat** [°dec] | **Lon** [° dec] | **PGA** [g] | **$S_a$(T=0.3s)** [g] | **$S_a$(T=1s)** [g] | **$S_a$(T=3s)** [g] | **PGA** [g] | **$S_a$(T=0.3s)** [g] | **$S_a$(T=1s)** [g] | **$S_a$(T=3s)** [g] |
| MB 2.1 | 44.8870 | 11.0629 | 0.273 | 0.81 | 0.488 | 0.068 | 0.289 | 0.681 | 0.309 | 0.112 |
| MB 2.2 (a) | 44.8864 | 11.0644 | 0.282 | 0.841 | 0.508 | 0.070 | 0.286 | 0.680 | 0.308 | 0.112 |
| MB 2.2 (b) | 44.8850 | 11.0663 | 0.284 | 0.852 | 0.516 | 0.071 | 0.283 | 0.676 | 0.310 | 0.117 |
| MB 2.2 (c) | 44.8395 | 11.1400 | 0.309 | 0.849 | 0.538 | 0.067 | 0.293 | 0.828 | 0.290 | 0.093 |
| MB 2.3 C1 | 44.8860 | 11.0665 | 0.283 | 0.846 | 0.511 | 0.071 | 0.286 | 0.681 | 0.301 | 0.111 |
| MB 2.3 C2 | 44.8635 | 11.0775 | 0.295 | 0.844 | 0.502 | 0.068 | 0.309 | 0.739 | 0.295 | 0.110 |
| PCB 3.5 | 44.8471 | 11.2084 | 0.304 | 0.716 | 0.425 | 0.051 | 0.296 | 0.867 | 0.250 | 0.061 |
| PCBs 3.1,3.2 | 44.8255 | 11.0394 | 0.196 | 0.534 | 0.311 | 0.046 | 0.282 | 0.653 | 0.271 | 0.106 |
| PCBs 3.3,3.4 | 44.8403 | 11.0568 | 0.230 | 0.635 | 0.37 | 0.053 | 0.294 | 0.694 | 0.279 | 0.107 |
| RCB 4.1 | 44.8858 | 11.0653 | 0.283 | 0.846 | 0.512 | 0.071 | 0.286 | 0.680 | 0.308 | 0.112 |
| RCB 4.2 | 44.8839 | 11.0655 | 0.285 | 0.858 | 0.521 | 0.072 | 0.283 | 0.677 | 0.311 | 0.117 |

It is worth noting that the area of interest is mostly characterized by soft soil classes C and D (Verderame et al., 2012). Further information about ground motion characteristics of the two events can be found in Chioccarelli et al. (2012a, 2012b).

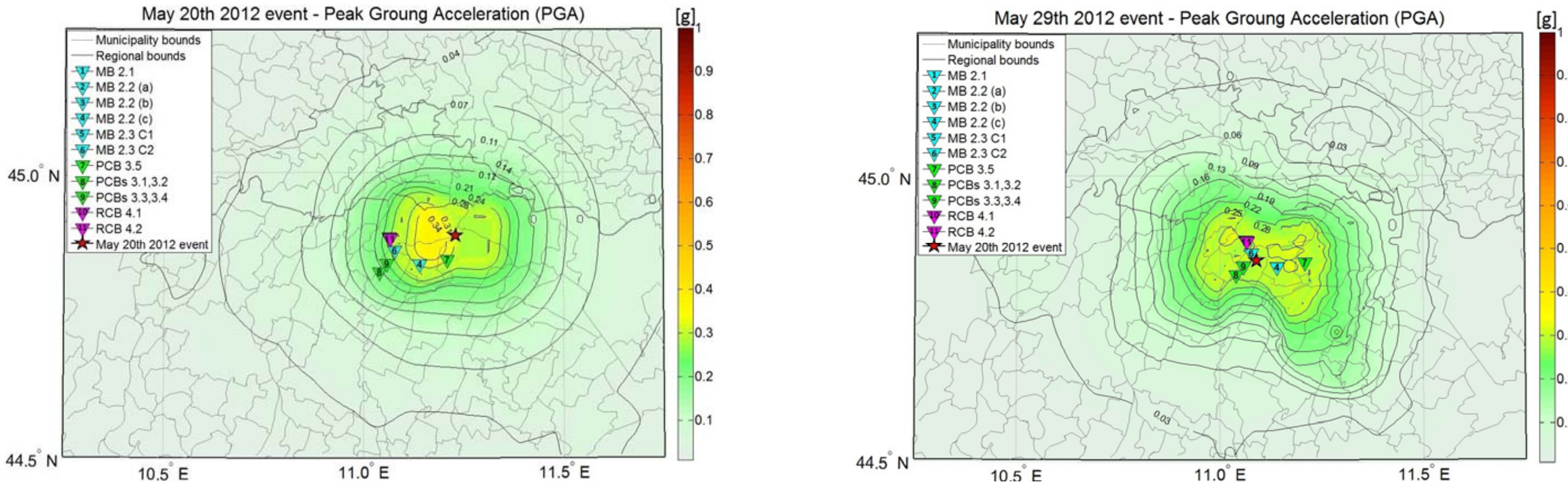


(a) (b)

**Figure 1.2.** Shaking maps in terms of PGA: (a) May 20th event; (b) May 29th event.

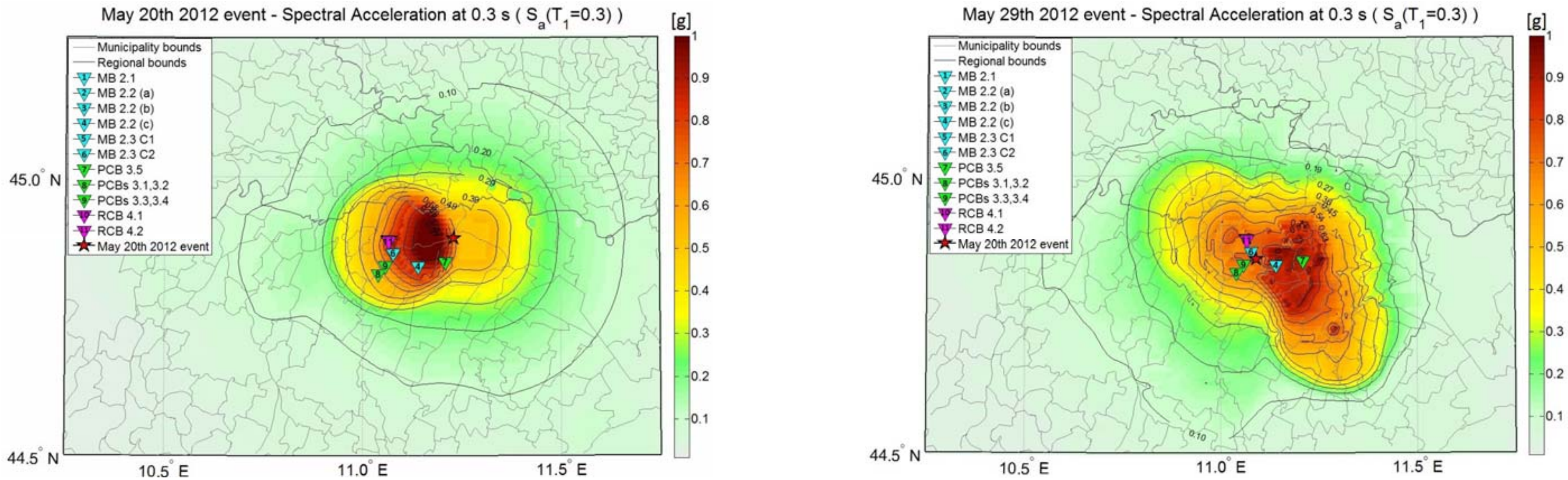


(a) (b)

**Figure 1.3.** Shaking maps in terms of $S_a(T = 0.3\ \text{s})$: (a) May 20th event; (b) May 29th event.

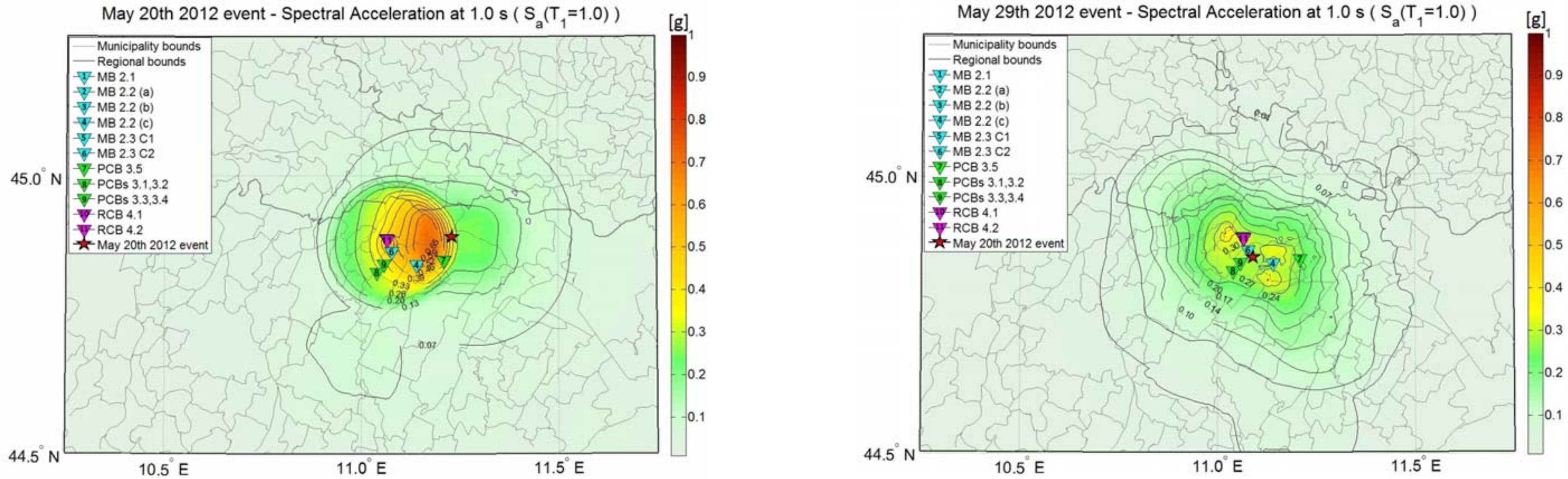


(a) (b)

**Figure 1.4.** Shaking maps in terms of $S_a(T = 1.0\text{ s})$: (a) May 20th event; (b) May 29th event.

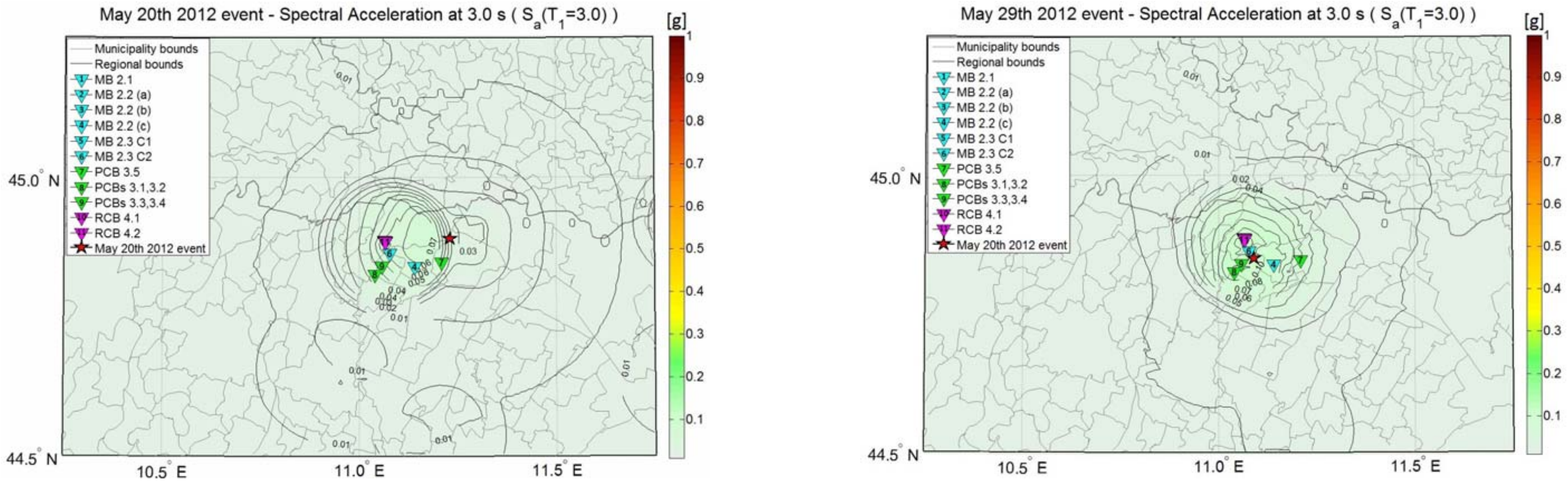


(a) (b)

**Figure 1.5.** Shaking maps in terms of $S_a(T = 3.0\text{ s})$: (a) May 20th event; (b) May 29th event.

# 2. Damage to masonry buildings

## *2.1. Modern residential buildings*

(a) (b)

**Figure 2.1.** Brick masonry buildings in Mirandola (Lat. 44.886969, Lon. 11.062936): Out-of-plane failures of walls due to lack of roof-to-wall connections (e.g., RC ring beams, wooden or steel ties, reinforced masonry stringcourses).

(a) (b)

**Figure 2.2.** In-plane diagonal shear cracks of spandrel panels of brick masonry buildings located in Mirandola (Lat. 44.886969, Lon. 11.062936): (a) Floor level; (b) Roof level.

*2.2. Historic building aggregates*

(a) (b)

**Figure 2.3.** Global collapse of corner building unit in Mirandola (Lat. 44.886417, Lon. 11.064429): (a) General view; (b) Temporary shoring system supporting the adjacent multi-leaf masonry building unit.

(a) (b)

**Figure 2.4.** Building aggregate in Mirandola (Lat. 44.884998, Lon. 11.066348): (a) Beginning of corner failure mechanism; (b) Beginning of vertical overturning mechanism due to bad corner connection.

(a) (b)

**Figure 2.5.** Partial collapse of corner brick masonry building unit in San Felice sul Panaro (Lat. 44.839492, Lon. 11.140061): (a) View of collapsed corner; (b) Opposite view.

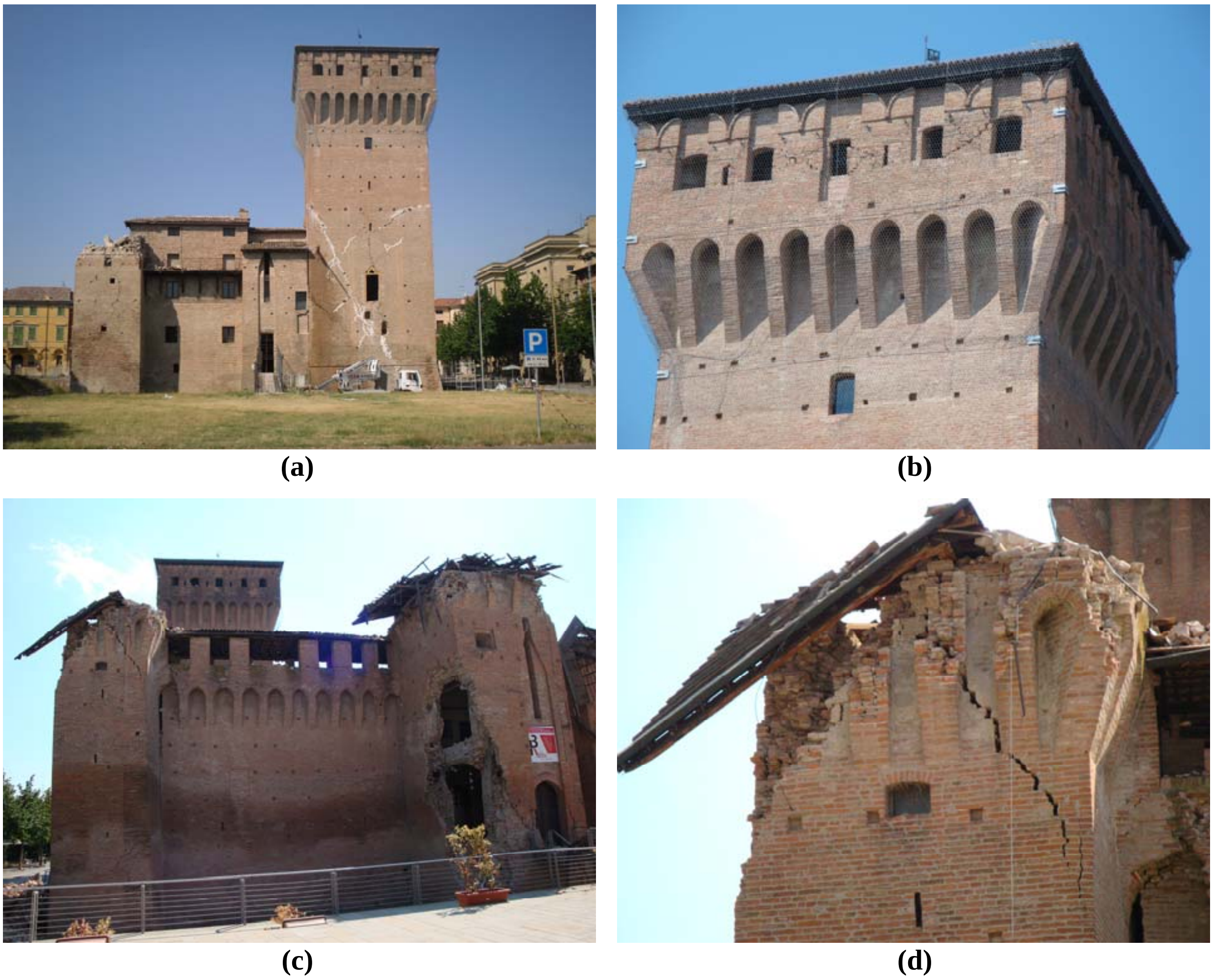

(a) (b) (c) (d)

**Figure 2.6.** Heavy damage to the Castle of San Felice sul Panaro (Lat. 44.839492, Lon. 11.140061): (a) Totally collapsed left tower on lateral façade and diagonal cracks on the right tower due to torsion; (b) Detail of shear damage to the upper part of the right tower; (c) Main façade; (d) Detail of damage to the upper part of the left tower on the main façade.

## 2.3. Churches

(a) (b)

**Figure 2.7.** Cathedral of Santa Maria Maggiore in Mirandola (Lat. 44.886027, Lon.11.066543): (a) Front view of the brick masonry structure (Note the collapse of tympanum due to out-of-plane seismic excitation.); (b) Diagonal cracks of bell tower.

(a) (b)

**Figure 2.8.** Brick masonry church in Mirandola (Lat. 44.863452, Lon. 11.077511): (a) Out-of-plane partial collapse of main façade; (b) Corner view.

**(a)** **(b)**

**Figure 2.9.** Brick masonry church in Mirandola (Lat. 44.863452, Lon. 11.077511): (a) Out-of-plane partial collapse of lateral façade (Note the rupture of steel tie below the level of the wooden truss support.); (b) Partially collapsed bell tower.

# 3. Damage to industrial buildings

## *3.1. Precast RC building in Cavezzo*

**Figure 3.1.** External view of the building (Lat. 44.825486, Lon. 11.039357). Overturning mechanism of vertical façade precast concrete (PC) panels.

**Figure 3.2.** Detail of vertical façade PC panel (Lat. 44.825486, Lon. 11.039357).

**(a)**

**(b)**

**Figure 3.3.** Connections of vertical façade PC panels to (a) floor and (b) ground (Lat. 44.825486, Lon. 11.039357).

**(a)** **(b)**

**Figure 3.4.** (a) Precast roof slab elements; (b) internal view of collapsed part of the building (Lat. 44.825486, Lon. 11.039357).

**(a)** **(b)**

**Figure 3.5.** Vertical seismic joint: (a) View; (b) Measurement (Lat. 44.825486, Lon. 11.039357).

**(a)** **(b)**

**Figure 3.6.** (a) Rupture of U-shaped seat on RC column; (b) Collapsed roof beam with U-shaped cross section (Lat. 44.825486, Lon. 11.039357).

*3.2. Precast RC building in Cavezzo*

(a) (b)

**Figure 3.7.** (a) Internal view of damaged building; (b) Detachment of façade from orthogonal partition wall due to out-of-plane earthquake excitation (Lat. 44.825486, Lon. 11.039357).

(a) (b) (c)

**Figure 3.8.** Buckling of longitudinal reinforcing steel bar due to biaxial bending (stirrup spacing was found to be about 200 mm) (Lat. 44.825486, Lon. 11.039357).

**(a)** **(b)**

**Figure 3.9.** (a) Ejected cover at opposite column corners due to biaxial bending; (b) Ejected cover at the same column edge due to uniaxial bending (Lat. 44.825486, Lon. 11.039357).

## *3.3. Precast RC building in Medolla*

**Figure 3.10.** Temporary safety measures to avoid out-of-plane rotation of roof beams (Lat. 44.840301, Lon. 11.056790).

**Figure 3.11.** Internal view of collapsed ceilings (Lat. 44.840301, Lon. 11.056790).

**Figure 3.12.** Cracks at column base (Lat. 44.840301, Lon. 11.056790).

**Figure 3.13.** Detail of failed connection of façade panel to the structure (Lat. 44.840301, Lon. 11.056790).

### *3.4. Precast RC building in Medolla*

**Figure 3.14.** Safety measures to avoid façade overturning (Lat. 44.840301, Lon. 11.056790).

(a) (b)

**Figure 3.15.** Deformed configuration of steel scaffolding system (Lat. 44.840301, Lon. 11.056790).

**Figure 3.16.** Rupture of steel diagonal in proximity of bracing joint (Lat. 44.840301, Lon. 11.056790).

(a) (b)

**Figure 3.17.** Connection of scaffolding column to the ground (Lat. 44.840301, Lon. 11.056790).

*3.5. Precast RC building in San Felice sul Panaro*

**Figure 3.18.** External view (Lat. 44.847060, Lon. 11.208389).

**(a)** **(b)** **(c)**

**Figure 3.19.** (a) Column damaged as a result of outward rotation; (b) damage to external beam-column joint; (c) damage close to beam seat (Lat. 44.847060, Lon. 11.208389).

**(a)** **(b)**

**Figure 3.20.** (a) General view and (b) detail of collapsed PC roof beam (Lat. 44.847060, Lon. 11.208389).

**Figure 3.21.** Detail of sandwich façade panels with RC cover (Lat. 44.847060, Lon. 11.208389).

# 4. Damage to reinforced concrete buildings

(a) (b)

**Figure 4.1.** Non-structural damage to RC building in Mirandola (Lat. 44.885774, Lon. 11.065298): (a) General view of the building; (b) Detail of diagonal shear cracking of solid brick masonry infill wall at the first floor and local crushing of infill wall at the ground floor, close to the beam-column joint.


(a) (b)

**Figure 4.2.** Non-structural damage to RC building in Mirandola (Lat. 44.885774, Lon. 11.065298): (a) Local crushing of hollow brick masonry infill wall at the interface with RC columns of ground floor; (b) Detail of shear cracking of RC column due to column-wall interaction under horizontal seismic actions.

**(a)** **(b)**

**Figure 4.3.** Damage to RC building in Mirandola (Lat. 44.885774, Lon. 11.065298): (a) Corner view; (b) Detail of local crushing of hollow brick masonry infill wall.

**(a)** **(b)**

**Figure 4.4.** Structural damage to RC building in Mirandola (Lat. 44.885774, Lon. 11.065298): (a) Failure of columns due to interaction with partial infill wall; (b) Shear crack with typical diagonal shear crack in corner column.

**(a)** **(b)**

**Figure 4.5.** Structural damage to RC building in Mirandola (Lat. 44.885774, Lon. 11.065298): (a) Damage with large diagonal shear crack in intermediate column; (b) Buckling of longitudinal steel bar in intermediate column.

**(a)** **(b)**

**Figure 4.6.** Non-structural damage to RC building in Mirandola (Lat. 44.885774, Lon. 11.065298): (a) Collapsed panel above large opening at the ground floor; (b) Diagonal shear cracks in solid brick masonry infill wall.

**(a)** **(b)**

**Figure 4.7.** Damage to RC building in Mirandola (Lat. 44.883916, Lon. 11.065483).

**(a)** **(b)**

**Figure 4.8.** Damage to RC building in Mirandola (Lat. 44.883916, Lon. 11.065483): (a) Early shear cracking of deep beams; (b) Partial external leaf detachment of solid bricks infill wall.

## 5. Summary of post-earthquake reconnaissance activity

The surveyed buildings in the previous sections emphasize typical weaknesses of different structural typologies in areas recently classified as seismically prone. Other examples of damage can be found in a number of reconnaissance reports already available (EPICentre Field Observation Report No. EPI-FO-200512, 2012; EPICentre Field Observation Report No. EPI-FO-290512, 2012; Decanini et al., 2012). The damages described in this report allow the authors to point out that:

(1) The Emilia Romagna earthquakes mainly destroyed masonry and RC precast buildings. In both cases the observed structural damage was mostly caused by lack of proper connection detailing.

(2) Out-of-plane failure modes can affect not only historical masonry buildings as observed after other damaging earthquakes (see for instance Augenti and Parisi, 2010), but also modern masonry buildings which do not have a satisfactory masonry interlocking between orthogonal load-bearing walls and effective connections between floors and walls (e.g., RC bond beams, steel ties). Corner units of masonry building aggregates, which are very spread in Italy and Europe, are significantly prone to suffer local collapse mechanisms, because they are not confined on both sides by adjacent building units. Finally, it was again confirmed the high vulnerability level of tympanums and bell towers of masonry churches, which typically experience local collapse mechanisms under bending and torsion, respectively.

(3) In-plane earthquake damage to piers and spandrels of masonry buildings was another typical failure mode which can also occur in modern masonry buildings and consist of complex crack patterns in the case of masonry walls with irregular layout of openings (Parisi and Augenti, in press).

(4) Most of RC residential buildings suffered damage non-structural components. Local interaction between masonry infills (with or without openings) and RC columns was the main cause of the observed structural damage (Verderame et al., 2011).

(5) The majority of heavy damaged or collapsed industrial buildings were designed for gravity loads only. Lacking or ineffective connections between RC precast roof beams and columns induced partially constrained roof systems which slipped off under large relative displacements between top sections of columns. Ineffective connections between vertical façade panels and the structure caused dangerous out-of-plane collapse mechanisms of the panels.

## Acknowledgements

This study was carried out in the framework of the ReLUIS-DPC 2010–2013 research project under funding of the Italian Civil Protection Department. The authors thank Dr. Luigi Di Sarno for his precious support in the field mission.

## References

Augenti N., Parisi F. (2010). Learning from construction failures due to the 2009 L'Aquila, Italy, earthquake. Journal of Performance of Constructed Facilities, 24(6), pp. 536-555.

Chioccarelli E., De Luca F., Iervolino I. (2012a). Preliminary study of Emilia (May 20th 2012) earthquake ground motion records, v2.11 [available at http://www.reluis.it].

Chioccarelli E., De Luca F., Iervolino I. (2012b). Preliminary study of Emilia (May 29th 2012) earthquake ground motion records, v1.0 [available at http://www.reluis.it].

Decanini L., Liberatore D., Liberatore L., Sorrentino L. (2012). Preliminary report on the 2012, May 20th, Emilia earthquake, v1.0 [available at http://www.eqclearinghouse.org/2012-05-20-italy-it/files/2012/06/Emilia2012_DecaniniLiberatoreLiberatoreSorrentino_v1.pdf].

EPICentre Field Observation Report No. EPI-FO-200512 (2012). The 20th May 2012 EmiliaRomagna Earthquake [available at http://www.ucl.ac.uk/~ucestor/research-earthquake/EPICentre_Report_EPIFO-200512-v2.pdf].

EPICentre Field Observation Report No. EPI-FO-290512 (2012). The 29th May 2012 EmiliaRomagna Earthquake [available at http://www.ucl.ac.uk/~ucestor/research-earthquake/EPICentre_Report_EPIFO-290512.pdf].

Italian Building Code (2008). DM 14.01.2008: Norme Tecniche per le Costruzioni. Italian Ministry of Infrastructures and Transportation, Rome, Italy.

Parisi F., Augenti N. (in press). Seismic capacity of irregular unreinforced masonry walls with openings. Earthquake Engineering and Structural Dynamics.

Verderame G.M., De Luca F., De Risi M.T., Del Gaudio C., Ricci P. (2012). A three level vulnerability approach for damage assessment of infilled RC buildings: The Emilia 2012 case, v1.0 [available at http://www.reluis.it].

Verderame G.M., De Luca F., Ricci P., Manfredi G. (2011). Preliminary analysis of a soft-storey mechanism after the 2009 L'Aquila earthquake. Earthquake Engineering and Structural Dynamics, 40(8), pp. 925-944.